Angular Distributions from Multiparticle Production Models*

DONALD E. LYON, JR.
Department of Physics, University of Michigan, Ann Arbor, Michigan 48104

AND

CLIFFORD RISK AND DON M. TOW
Lawrence Radiation Laboratory, University of California, Berkeley, California 94720

(Received 27 July 1970)

Using $\exp(-Ap_T^2)d^3p/E$ as the momentum distribution of secondaries produced in ultrahigh-energy collisions—a result predicted by the multiperipheral model, by Feynman's parton model, and by Cheng and Wu's consideration of hadrons as extended objects with many internal degrees of freedom—we obtain the characteristic features of the angular distribution. We discuss the dependence on incident energy, mass of secondaries, and the value of A. We find that the c.m. angular distribution on the variable $\eta_{\text{c.m.}} = -\ln \tan\frac{1}{2}\theta_{\text{c.m.}}$ has a two-bump structure, whereas the lab angular distribution in $\eta = -\ln \tan\theta_l$ is flat. This difference leads us to a discussion of the transformation between c.m. and lab angular distributions. We find that the usual relativistic approximation of the exact transformation leads to incorrect results. Finally, we point out that these momentum and angular distributions approach limiting distributions.

IN the last two years advances have been made in the development of theoretical models of multiparticle production in high-energy collisions. The multiperipheral model (MPM) of ABFST[1] has been revived and studied in the form with elementary pion exchange[2] as well as the form with Reggeized meson exchange.[3] Further developments have been made by Feynman[4] with his parton model, and by Cheng and Wu[5] through the study of Feynman diagrams. At the same time, the Michigan-Wisconsin collaboration[6] has collected ≈ 800 interactions of cosmic-ray hadrons in liquid hydrogen, in the range 100–800 GeV. Among other things, they measured the angular distribution of the produced secondaries.[7] These new data have offered the opportunity to test the predictions made by these models regarding angular distributions. In an earlier work[8] this test was performed. In this paper we explore in detail the characteristic features of the angular distribution predicted by these theoretical models.

Rather than be constrained by the specific features of any one model, we discuss the general features common to all three models. They all predict that the momentum distribution of the secondaries is given by[9]

$$d^3N = e^{-Ap_T^2}(d^3p/E), \tag{1a}$$

and hence that the double-differential momentum distribution is given by

$$\frac{\partial^2 N}{\partial p_L \partial p_T} = \frac{p_T e^{-Ap_T^2}}{(p_L^2 + p_T^2 + m^2)^{1/2}}. \tag{1b}$$

Here p_L and p_T are the longitudinal and transverse momentum components of the secondary, m is its mass, and E is its energy. Of course, this distribution does not hold for all secondary momenta up to the kinematical boundary because of phase-space effects. The over-all δ function of energy-momentum conservation modifies the distribution near the boundary, and, hence, Eq. (1) holds only for secondaries sufficiently far from it. For example, in the center-of-momentum system [see Fig. 1(a)] we expect the distribution (1) to hold inside the region 2-3, with modifications outside. In the laboratory system [see Fig. 1(b)] we expect the distribution (1) to hold inside the region 2′-3′, with modifications outside. [We emphasize that (1) holds only for the produced secondaries; the incident particle, which has an elasticity ≈ 0.5, must be handled separately.]

It is not hard to anticipate the general features of the angular distribution predicted by Eq. (1). In the lab

* Work supported by the U. S. Atomic Energy Commission and the National Science Foundation.

[1] L. Bertocchi, S. Fubini, and M. Tonin, Nuovo Cimento 25, 626 (1962); D. Amati, A. Stanghellini, and S. Fubini, *ibid.* 26, 896 (1962).

[2] J. S. Ball and G. Marchesini, Phys. Rev. 188, 2508 (1969); D. M. Tow, Phys. Rev. D 2, 154 (1970); G. F. Chew, T. W. Rogers, and D. R. Snider, *ibid.* 2, 765 (1970).

[3] See, e.g., G. F. Chew and A. Pignotti, Phys. Rev. 176, 2112 (1968); G. F. Chew, M. L. Goldberger, and F. E. Low, Phys. Rev. Letters 22, 208 (1969); I. G. Halliday, Nuovo Cimento 60A, 177 (1969); I. G. Halliday and L. M. Saunders, *ibid.* 60A, 494 (1969); P. D. Ting, LRL Report No. UCRL-19802, 1970 (unpublished).

[4] R. P. Feynman, in *Proceedings of the Third International Conference High-Energy Collisions, Stony Brook, 1969*, edited by C. N. Yang *et al.* (Gordon and Breach, New York, 1969).

[5] H. Cheng and T. T. Wu, Phys. Rev. Letters 23, 1311 (1969).

[6] K. N. Erickson, thesis, Colorado State University, 1970 (unpublished); and L. W. Jones *et al.*, report presented at the sixth Interamerican Seminar on Cosmic Rays, La Paz, Bolivia, 1970 (unpublished).

[7] Until now the only source of angular distributions from ultrahigh-energy collisions has been from the interactions of cosmic-ray hadrons with complex nuclei. However, this type of experiment has produced only a small number of events suitable for analysis, and these were obtained without a direct measurement of the incident energy.

[8] L. Caneschi, D. E. Lyon, Jr., and Clifford Risk, Phys. Rev. Letters 25, 774 (1970).

[9] These three models actually predict $d^3N = f(p_T^2)d^3p/E$. However, Tow, in Ref. 2, has shown numerically for the ABFST multiperipheral model that $f(p_T^2)$ is of the form $\exp(-Ap_T^2)$ (here we have ignored the small second bump in the p_T distribution found in this paper.)

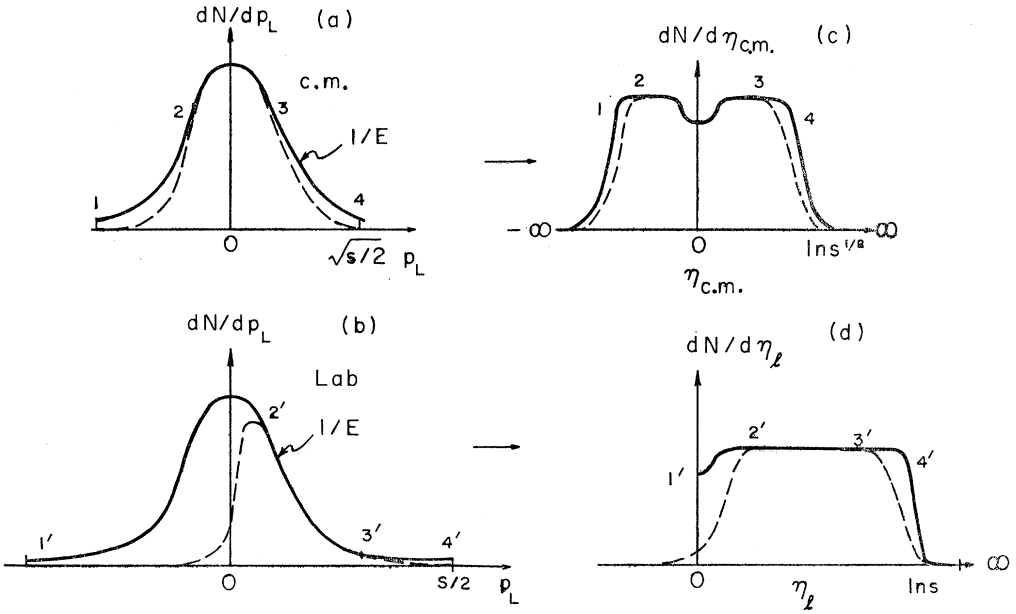

FIG. 1. Longitudinal momentum and angular distributions. Solid lines are predictions of Eq. (1) without phase-space corrections; dashed lines include phase-space corrections. (a) $dN/dp_L=1/E$ in c.m., (b) $dN/dp_L=1/E$ in lab, (c) $dN/d\eta_{\text{c.m.}}$, and (d) $dN/d\eta_l$.

system Eq. (1) is valid over some range $0\ll p_L\ll p_{\max}{}^l \approx \frac{1}{2}s$, where s is the c.m. energy squared. Since the transverse momentum distribution is peaked about some small value p_{T0}, and since in the lab $p_L\gg p_{T0}$, the lab angle θ_l of emission of secondaries relative to the beam direction will be predominantly small. This leads us to use the variable η:

$$\eta\equiv-\ln\tan\theta_l = \ln(p_L/p_T)\approx\ln(p_L/p_{T0}), \quad (2)$$

which stretches the θ_l axis in the region of interest.[10] Then, noting that in the lab system $p_L\approx E$ for the secondaries in the range of validity of Eq. (1), we obtain

$$\frac{\partial N}{\partial\eta}\approx\frac{\partial N}{\partial[\ln(p_L/p_{T0})]}=p_L\frac{\partial N}{\partial p_L}\approx\text{const.}$$

Therefore, the η distribution is flat over the range of η corresponding to the p_L from region 2′-3′ of Fig. 1(b), and drops to zero on either side.

In the center-of-momentum system, Eq. (1) is valid over the symmetric region $|p_L|\ll p_{\max}{}^c\approx\frac{1}{2}s^{1/2}$, and the peaking of p_T now leads predominantly to forward-backward emission. Hence we use the variable $\eta_{\text{c.m.}}$,

$$\eta_{\text{c.m.}}\equiv-\ln\tan\tfrac{1}{2}\theta_{\text{c.m.}}, \quad (3)$$

where $\theta_{\text{c.m.}}$ is the c.m. angle of emission of secondaries relative to the beam. The regions $p_L\approx\pm E$ now give two flat sections in the $\eta_{\text{c.m.}}$ distribution that are located on either side of $\eta_{\text{c.m.}}=0$ ($\theta_{\text{c.m.}}=90°$), with some other behavior around $\eta_{\text{c.m.}}=0$. For $\eta_{\text{c.m.}}$ near the kinematical boundary, the distribution drops to zero.

[10] In the lab system almost all events lie within 90° of the beam direction.

These general features can be seen in detail by deriving a closed form for the angular distribution. We begin with the center-of-momentum system, and, as a first approximation, we neglect the phase-space modifications to Eq. (1). Changing variables to $p=(p_L{}^2+p_T{}^2)^{1/2}$ and $\eta_{\text{c.m.}}$, we obtain from Eq. (1b)

$$\frac{dN}{d\eta_{\text{c.m.}}}=\frac{1}{\cosh^2\eta_{\text{c.m.}}}\int_0^{p_{\max}{}^{\text{c.m.}}}\frac{p^2}{(p^2+m^2)^{1/2}}\times\exp\left(\frac{-Ap^2}{\cosh^2\eta_{\text{c.m.}}}\right)dp. \quad (4)$$

Integration leads to

$$\frac{dN}{d\eta_{\text{c.m.}}}=\frac{1}{2A}\{xe^x[K_1(x)-K_0(x)]-\exp[-2x(p_{\max}{}^{\text{c.m.}}/m)^2]\}, \quad (5)$$

where $x=\frac{1}{2}(m^2A/\cosh^2\eta_{\text{c.m.}})$ and K_0, K_1 are modified Hankel functions. For large $\eta_{\text{c.m.}}$ (but small enough so that $e^x\gg\exp[-2x(p_{\max}{}^{\text{c.m.}}/m)^2]$), K_1 dominates Eq. (5) and gives a flat distribution, independent of m. When $\cosh^2\eta_{\text{c.m.}}\approx A(p_{\max}{}^{\text{c.m.}})^2$ [i.e., when $\eta_{\text{c.m.}}\approx\ln(A^{1/2}p_{\max}{}^{\text{c.m.}})$], the first and third terms cancel and the distribution drops to zero. The width of the distribution is therefore proportional to $\ln p_{\max}{}^{\text{c.m.}}$ or to $\ln s$. Figure 2(a) shows the $\eta_{\text{c.m.}}$ distribution for several values of $p_{\max}{}^{\text{c.m.}}$, with A and m fixed, and Figs. 2(b) and 2(c) illustrate the dependence on A and m when $p_{\max}{}^{\text{c.m.}}$ is fixed. We see that the distribution has a two-bump structure, with the dip at $\eta_{\text{c.m.}}=0$ proportional to A and m. Finally, from Fig. 1(a) we know that the correct distribution (with phase-space

effects included) deviates from Eq. (5) for large $|\eta_{c.m.}|$ (i.e., for large $|p_L|$); but the deviations occur at the ends of the distribution and do not change the shape of the internal portion [see Fig. 1(c)].

In the lab system, because Eq. (1) is invariant under a z boost (z is the beam direction), the distribution in the lab variable $\eta_l \equiv -\ln \tan\frac{1}{2}\theta_l$ is again given by Eq. (4):

$$\frac{dN}{d\eta_l} = \frac{1}{\cosh^2\eta_l}\int_0^{p_{\max}{}^l} \frac{p^2}{(p^2+m^2)^{1/2}} \exp\left(\frac{-Ap^2}{\cosh^2\eta_l}\right)dp. \quad (4')$$

However, as previously discussed, the energy-momentum conservation δ function now restricts the region of validity of Eq. (1) to some positive range (i.e., $\eta_l > 0$), so that the η_l distribution is just the right-hand portion of the $\eta_{c.m.}$ distribution, stretched by the larger $p_{\max}{}^l \approx \frac{1}{2}s$. Here the phase-space effects cause the correct distribution to deviate from Eq. (4') in the regions of small p_L and very large p_L (i.e., for $\eta_l \approx 0$ and large η_l). The η_l distribution is therefore a single-bump distribution [see Fig. 1(d)]. The $\eta \equiv -\ln \tan\theta_l$ distribution, which is related to the η_l distribution by a Jacobian

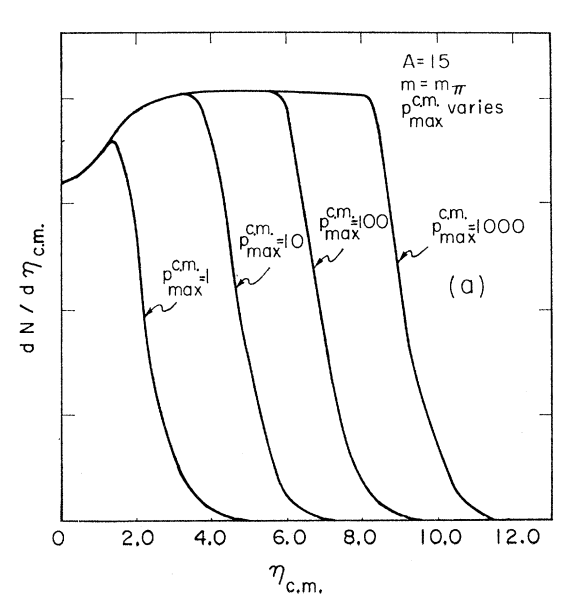

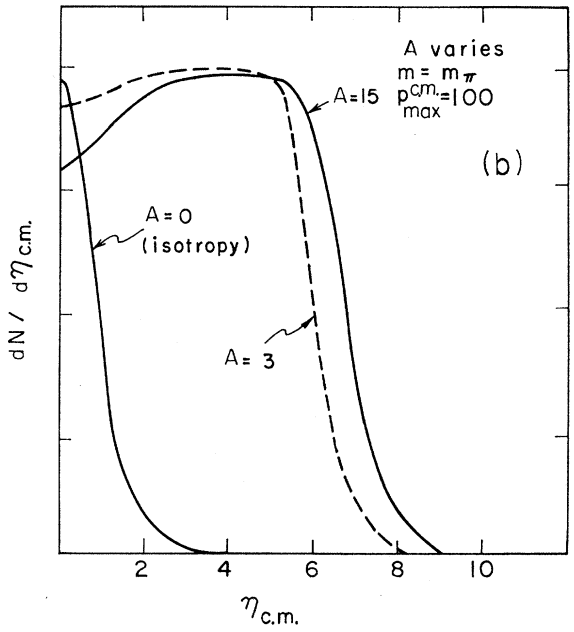

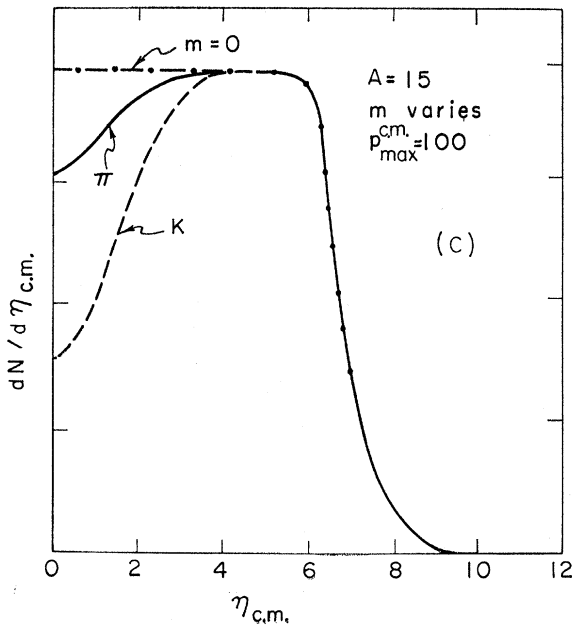

FIG. 2. $dN/d\eta_{c.m.}$ plot. The distribution is symmetric about $\eta_{c.m.}=0$. (a) $p_{\max}{}^{c.m.}$ varies, A and m are fixed; (b) A varies, $p_{\max}{}^{c.m.}$ and m are fixed; (c) m varies, $p_{\max}{}^{c.m.}$ and A are fixed.

that effectively stretches the η_l axis, is then also a single-bump distribution (see Fig. 3).[11]

The difference between the $\eta_{\text{c.m.}}$ and η distributions (the two-bump structure of $dN/d\eta_{\text{c.m.}}$ and the single-bump structure of $dN/d\eta$) shows that a relativistic approximation that has often been used to transform angular distributions from lab system to c.m. system can give misleading results. This transformation states that the $dN/d\eta$ and $dN/d\eta_{\text{c.m.}}$ distributions are related by a simple translation of the η axis by an amount $\ln\gamma$. This comes about in the following way: The angles θ_l and $\theta_{\text{c.m.}}$ are related by

$$\tan\theta_l = \frac{1}{\gamma_c}\frac{\sin\theta_{\text{c.m.}}}{(\cos\theta_{\text{c.m.}}+\beta_c/\beta)}, \tag{6}$$

where β is the velocity of the secondary in the c.m. system and β_c is the velocity of the c.m. system relative to the lab system $[\gamma_c=(1-\beta_c^2)^{-1/2}]$. For large incident energy, $\beta_c\approx 1$; if the secondary is also relativistic, then $\beta\approx 1$ and one obtains

$$\tan\theta_l \xrightarrow[\beta_c/\beta\to 1]{} \frac{1}{\gamma_c}\tan\tfrac{1}{2}\theta_{\text{c.m.}} \tag{7a}$$

or

$$\eta = \ln\gamma_c + \eta_{\text{c.m.}}. \tag{7b}$$

However, from our derivations of the correct distributions [Figs. 2(a) and 3], we know that this transformation cannot be valid. This can be understood by examining a c.m. Peyrou plot generated from the distribution (1) (see Fig. 4). Note that in this plot many secondaries populate the region near the origin, and hence are nonrelativistic. The relativistic transformation (7) cannot hold for them; they must be transformed by the exact transformation (6).

Cosmic-ray physicists experimentally measure the angular distribution (lacking momentum analysis) of secondaries in the lab; then they often use the transformation (7) to get the "experimental" c.m. angular distribution and compare with various theoretical models. As we have shown, this relativistic transformation is a poor approximation. Therefore, a better approach is to develop theoretical models in the lab and compare directly with the measured lab data. If some theoretical models, such as the two-fireball model,[12] are most naturally formulated in the c.m. system, then one should transform to the lab system without using this relativistic approximation. One method is to specify the c.m. momentum distribution in the model, and transform it exactly into the lab system by Eq. (6). For example, in Ref. 8, the c.m. momentum distribution was determined by a Monte Carlo procedure, and the individual secondaries generated were transformed into the lab system by Eq. (6).

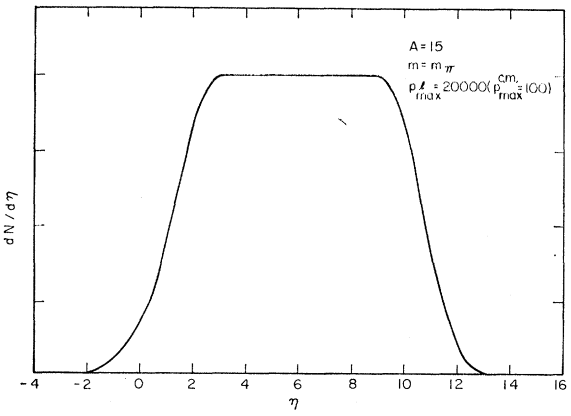

FIG. 3. $dN/d\eta$ plot.

The possibility of a simple transformation between the lab and c.m. systems is retained by using a variable w, called rapidity, which was recently introduced by Feynman[4]:

$$w=\tanh^{-1}\left(\frac{p_L}{E}\right)=-\ln\left[\frac{E-p_L}{(p_T^2+m^2)^{1/2}}\right]. \tag{8}$$

This variable satisfies

$$w_{\text{c.m.}}=-\ln\left(\frac{1-\beta}{1+\beta}\right)^{1/2}+w_{\text{lab}}. \tag{9}$$

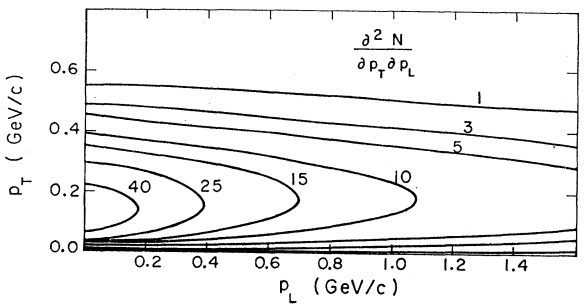

FIG. 4. Peyrou plot in c.m. system. Lines are level curves of constant density; numbers denote densities of particles per unit area along each curve.

[11] This flat lab distribution has raised doubt as to whether the multiperipheral model can explain the two-bump structure observed in some cosmic-ray events. However, O. Czyzewski and A. Krzywicki, Nuovo Cimento **30**, 603 (1963), using a flat distribution in η to generate events by a Monte Carlo method, found that the experimental two-bump structure can be explained as statistical fluctuations of the multiperipheral flat distribution. Recently, E. I. Daibog and I. L. Rozental, Yadern Fiz. **10**, 818 (1969) [Soviet J. Nucl. Phys. **10**, 473 (1970)], claimed that, using the momentum distribution $e^{-Bp_T}d^3p/p_L$, they get a two-bump distribution in the lab system. However, they incorrectly evaluated the Jacobian by replacing dp_L with dp. If they had not made this replacement, they would get essentially the same distribution as ours for the case $m=0$. They also claimed that Czyzewski and Krzywicki made a mistake in changing from p_L to p by neglecting the two-valued property of p_L. However Czyzewski and Krzywicki made this approximation in the lab system, where p_L, except for a very small fraction of particles, is always of the same sign.

[12] P. Ciok *et al.*, Nuovo Cimento **8**, 166 (1958); **10**, 741 (1958); G. Cocconi, Phys. Rev. **111**, 1699 (1958); K. Niu, Nuovo Cimento **10**, 944 (1958).

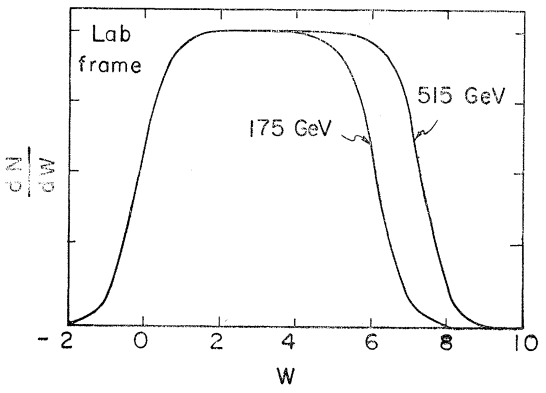

FIG. 5. dN/dw in lab system for two incident energies, with phase-space effects included by the method of Ref. 8. dN/dw in the c.m. system is related to the lab distribution through Eq. (9) by a translation.

(In the limit of $p_T^2 \gg m^2$, w reduces to $-\ln \tan\frac{1}{2}\theta$.) Using this variable and the distribution (1), we obtain a flat distribution for dN/dw in both the c.m. and the lab systems that scales with $\ln s$ (see Fig. 5). When experiments are done with storage rings or at the National Accelerator Laboratory, where momentum distributions can be measured, the Feynman rapidity variable should replace the usual $\ln \tan\theta$ variables.

Recently, Benecke, Chou, Yang, and Yen postulated the hypothesis of limiting fragmentation[13] which states that the momentum distribution of the fragments of the target (or projectile) approaches a limiting distribution in the lab system (or projectile system) as $s \to \infty$. Since the distribution (1) describes those secondaries with small p_L in the c.m. (so-called pionization products) and (1) is derived for large s and is independent of s, it implies that the momentum distribution of these pionization products approaches a limiting distribution in the lab system or any other system related to it by a z boost [the distribution (1) is invariant under z boost]. Furthermore, the momentum distribution (1) also leads to a limiting angular distribution; in Fig. 2(a) we see that the distributions, except for end effects, approach the same value. This approach to a limit at smaller η comes about from the sharp p_T cutoff of Eq. (1).

Note added in proof. After the completion of this paper, we received a report [D. Silverman and C.-I Tan, Princeton University report (unpublished)] which shows that, rigorously speaking, for general multiperipheral models the right-hand side of Eq. (1a) in general has an extra dependence on $x \equiv 2p_L^{\text{c.m}}/(s)^{\frac{1}{2}}$, where p_L and s are, respectively, the c.m. longitudinal momentum of the secondary and the c.m. energy squared. However, using an amplitude similar to the Chew-Pignotti multi-Regge amplitude (see Ref. 3) and treating phase space exactly, we have shown numerically that this x dependence is negligible for small values of x; this conclusion is also true in the more refined Caneschi-Pignotti multi-Regge model (see Ref. 8). Therefore, Eq. (1a) is a reasonable approximation to the true distribution predicted by the MPM. We thank Chung-I Tan for a correspondence clarifying this point.

[13] J. Benecke, T. T. Chou, C. N. Yang, and E. Yen, Phys. Rev. **188**, 2159 (1969).